Vortex structure and Josephson supercurrents in stacked double Josephson junctions

S. N. Song, P. R. Auvil, M. Ulmer, and J. B. Ketterson
Department of Physics and Astronomy and Materials Research Center, Northwestern University, Evanston, Illinois 60208
(Received 14 December 1995)

In Josephson-junction stacks consisting of two junctions having identical maximum Josephson supercurrent I_c, the measured I_c vs external magnetic flux Φ characteristics exhibit two distinct oscillation periods with the oscillation period for $\Phi>\Phi_0$ being smaller than that when $\Phi<\Phi_0$, where Φ_0 is the flux quantum. The observations provide clear evidence that a structural phase transformation to a triangular vortex lattice occurs with increasing Φ.

In a single Josephson junction, the Josephson vortices (fluxons) form a one-dimensional (1D) periodic lattice and, consequently, modulate the current density distribution within the junction. For a small, single Josephson junction, the Josephson supercurrent, I_c, vs applied magnetic field, H, has the familiar Fraunhofer diffraction behavior; i.e.,[1]

$$I_c = I_c(0)|\sin y/y|. \tag{1}$$

Here $y=\pi H/H_0=\pi\Phi/\Phi_0$, $\Phi=\mu_0 d_0 L H$ is the flux threading the junction, $\Phi_0=\mu_0 d_0 L H_0$ is the flux quantum, $d_0=a+2\lambda_L$ is the magnetic length, a is the barrier thickness, λ_L is the London penetration depth, and L is the junction length in the direction perpendicular to the applied magnetic field. For a large Josephson junction having $L\gg 2\pi\lambda_J$ (λ_J being the Josephson penetration depth), I_c vs H characteristics deviating from the Fraunhofer diffraction pattern have been observed; the observed behavior can be well accounted for by the theory of Owen and Scalapino.[2]

Recent technological progress has made it possible to fabricate stacked Josephson junctions (SJJ) of high quality. One can then study vortex statics and dynamics in this layered superconducting structure. Fundamental studies of fluxon interactions in SJJ's should open a new field of the nonlinear physics and associated applications.[3,4] In particular, the possibility of phase-lock motion of fluxons in SJJ's suggests that an SJJ can function as an efficient radiation source in millimeter and submillimeter wave cryoelectronic circuits.[5–7] To understand the more complicated vortex dynamics in SJJ's, a knowledge of the vortex statics is essential. In this paper we present an observation of a structural phase transformation to a triangular lattice in stacked Nb/Al-AlO_x/Nb/Al-AlO_x/Nb double Josephson junctions.

Nb/(Al-AlO_x/Nb)$_N$ trilayers ($N=1$) and multilayers ($N=2$) were deposited on thermally oxidized (100) Si wafers by dc magnetron sputtering. The thicknesses of the Nb base layer, the Al over layer, and the Nb counter-electrode layer were 2000, 80, and 2000 Å, respectively. The thickness of the intermediate Nb layers, b, ranged from 100 to 400 Å. Using standard photolithography, cross-geometry junctions were patterned by combining selective Nb etching (with a CF_4 plasma) and selective Nb anodization.[8] The I-V curves were measured across the bottom and top electrodes using the four terminal technique in a LHe Dewer surrounded by μ metal and copper concentric shields. External noise sources were carefully screened by filters in series with the sample and magnet leads.

In what follows we present data taken on four samples. The sample specifications and the junction parameters are listed in Table I. Usually, for a stacked junction consisting of N junctions having different maximum Josephson supercurrents, N current steps, corresponding to I_c at zero voltage and I_{cn} at a bias voltage of $2n\Delta/e$ ($n=1,2,...,N-1$) respectively, occur in the I-V curve at zero magnetic field. By carefully controlling the oxidation parameters for the AlO_x barrier formation, we were able to make stacked double junctions with $I_c\cong I_{c1}$. The insets in Figs. 1 and 2 show the I-V curve measured at 4.2 K and zero applied magnetic field for samples A and B, respectively, both of which are two-junction stacks. The backward slope of the I-V curves at the sum gap voltages arises probably from the heating effect. As can be seen in the insets of Figs. 1 and 2, the Josephson supercurrents of both junctions in the stacks are essentially identical, resulting in simultaneous switching from the superconducting to the quasiparticle branches of the I-V curve. As we will see this condition is critical for observations to be discussed below. The I_c vs H dependence is shown in Fig. 1 for sample A and in Fig. 2 for sample B. The magnetic field was applied perpendicular to one junction edge and parallel to the barrier layer. From Fig. 1 we see that the measured I_c vs H characteristic exhibits two distinct oscillation periods; the oscillation period for $H>H_0$ is smaller than that when $H<H_0$, where H_0 is the characteristic magnetic field corresponding to the first current minima. These data cannot be represented by the Fraunhofer diffraction pattern calculated from Eq. (1) using $y=\pi H/H_0$ as shown by the dashed line in Fig. 1. Similar behavior has also been observed on sample B (see Fig. 2) and samples on other chips, the I-V

TABLE I. Sample specifications and the junction parameters at 4.2 K.

Sample	N	L μm	b Å	J_c A/cm^2	L/λ_J	η
A	2	20	300	1000	2.00	−0.68
B	2	50	300	700	4.15	−0.68
C	2	50	200	80	1.43	−0.77
D	1	50		640	3.33	

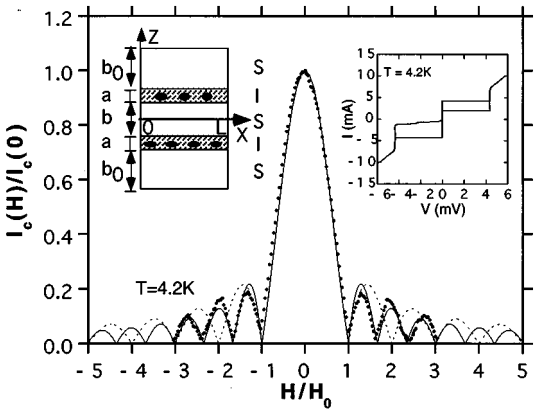

FIG. 1. The measured I_c vs H characteristics for sample A. The dashed line and the solid line are calculated from Eq. (1) using $y=\pi H/H_0$ and using Eq. (11), respectively (see the text). The right inset shows the I-V curve at 4.2 K and zero magnetic field; $\mu_0 H_0=0.78$ mT. The left inset shows a stacked double Josephson-junction structure schematically. Filled ellipses represent equilibrium fluxon positions of the vortex lattice in the two barriers.

curve of which also display the simultaneous switching behavior. For comparison, the measured I_c vs H characteristics for two more samples are shown in Fig. 3 (sample C) and Fig. 4 (sample D) which are from a two-junction stack and a single junction, respectively. The corresponding I-V curves at 4.2 K and zero magnetic field are shown as the insets in the figures. The inset of Fig. 3 shows that there is an additional current step occurring at a bias voltage of $2\Delta/e$, implying that the maximum Josephson supercurrents of the two junctions in this stack are not matched. The dashed lines in Figs. 3 and 4 are calculated from Eq. (1) using $y=\pi H/H_0$. Clearly, for these two samples the I_c vs H dependence can be described by Eq. (1) quite well.

From Table I we see that the length of all junctions studied here satisfies $L<2\pi\lambda_J$. Therefore, all of them are in the small junction limit, and finite-dimension effects may be neglected. Moreover, all the measured I_c vs H curves are symmetric about the vertical axis, hence the self-field effect is not important. The observed change in the oscillation period is therefore an intrinsic property associated with a transformation in the vortex structure in the matched, stacked double junctions. The validity of this conclusion is supported by the

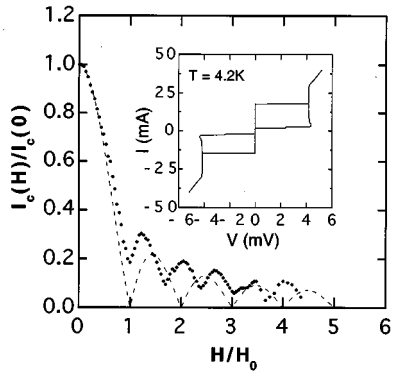

FIG. 2. The I_c vs H dependence for sample B. The dashed line is calculated from Eq. (1) using $y=\pi H/H_0$; $\mu_0 H_0=0.34$ mT. The inset shows the I-V curve at 4.2 K and zero magnetic field.

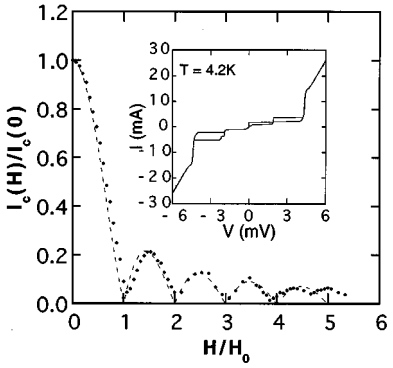

FIG. 3. The I_c vs H characteristics for sample C. The dashed line is calculated from Eq. (1) using $y=\pi H/H_0$. The inset shows the I-V curve at 4.2 K and zero magnetic field.

I_c vs H dependence of sample A measured at different temperatures (see Fig. 5). As seen in Fig. 5, while λ_J increases from about 10 μm at 4.2 K to 14 μm at 6.5 K, the oscillation behavior is essentially similar.

To understand the observed anomalous I_c vs H dependence, we consider a symmetric stacked double Josephson junction structure as shown schematically in the inset of Fig. 1. The structure consists of a base, middle, and top superconducting (S) layers of thickness b_0, b and b_0, and two insulating (I) barrier layers of thickness a, respectively. The coupled sine-Gordon (SG) equations describing the vortex statics in such a system are[3]

$$\frac{d^2\phi_1}{dX^2}=\frac{1}{\lambda_J^2}(\sin\phi_1+\eta\,\sin\phi_2), \tag{2a}$$

$$\frac{d^2\phi_2}{dX^2}=\frac{1}{\lambda_J^2}(\sin\phi_2+\eta\,\sin\phi_1). \tag{2b}$$

The coupling constant $\eta=s/d$ is determined by the thickness of the middle S layer, where the coupling parameter s is

$$s=-\lambda_L/\sinh(b/\lambda_L), \tag{3a}$$

the magnetic length d is

$$d=a+\lambda_L\coth(b/\lambda_L)+\lambda_L\coth(b_0/\lambda_L), \tag{3b}$$

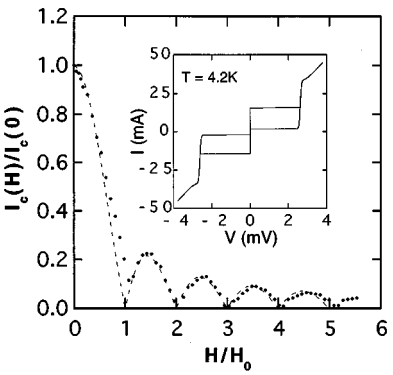

FIG. 4. The I_c vs H dependence for sample D. The dashed line is calculated from Eq. (1) using $y=\pi H/H_0$; $\mu_0 H_0=0.25$ mT. The inset shows the I-V curve at 4.2 K and zero magnetic field.

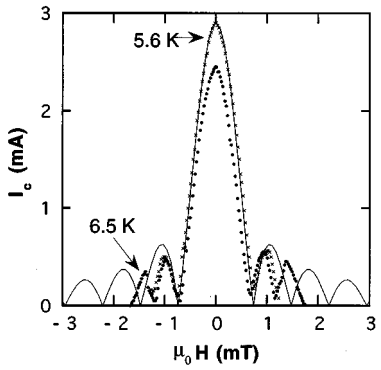

FIG. 5. The I_c vs H dependence for sample A at 5.6 and 6.4 K. The solid line is calculated from Eq. (1) using $y=\pi H/H_0$.

and the Josephson penetration depth is defined as

$$\lambda_J=(\Phi_0/2\pi\mu_0 dJ_c)^{1/2}, \tag{4}$$

where J_c is the maximum Josephson current density.

It is worth noting that Eqs. (2) have an exact solution for two special cases: $\phi_1=\phi_2$ (in phase) and $\phi_1=-\phi_2$ (out of phase). The corresponding magnetic lengths are[9]

$$d_+=d+s=a+\lambda_L\coth(b_0/\lambda_L)+\lambda_L\tanh(b/2\lambda_L), \quad \text{for } \phi_1=\phi_2 \tag{5a}$$

and

$$d_-=d-s=a+\lambda_L\coth(b_0/\lambda_L)+\lambda_L\coth(b/2\lambda_L), \quad \text{for } \phi_1=-\phi_2. \tag{5b}$$

A general solution corresponds to an effective magnetic length $d_{\rm eff}$ such that $d_+<d_{\rm eff}<d_-$. By examining the first integral of Eqs. (2), it is easy to verify that Eqs. (2) can be represented by the following Hamiltonian:

$$H=H_0+H_{\rm in}=\int_0^l\sum_{i=1}^{2}\left[\frac{1}{2}\left(\frac{d\phi_i}{dx}\right)^2+1-\cos\,\phi_i\right]dx-\eta\int_0^l\frac{d\phi_1}{dx}\frac{d\phi_2}{dx}\,dx, \tag{6}$$

where we have introduced the dimensionless coordinates $x=X/\overline{\lambda}_J$, $l=L/\overline{\lambda}_J$, and

$$\overline{\lambda}_J\equiv\lambda_J/(1-\eta^2)^{1/2}. \tag{7}$$

We emphasize that upon adding the kinetic energies, Eq. (6) [along with Eq. (7)] is the exact Hamiltonian describing the coupled sine-Gordon system. Similar equations were described earlier with the coupling constant introduced as a phenomenological parameter.[10–12] Since $d\phi_i/dx$ is directly related to the magnetic field, the coupling is essentially magnetic in nature.

In the absence of the coupling, each junction in the stack is described by the unperturbed sine-Gordon equation. An exact solution to the unperturbed SG equation describing the periodic 1D vortex lattice is[2]

$$\phi_i(x)=\pi-2\,\mathrm{am}\left(\frac{x-x_i^0}{k},k\right), \quad (i=1,2) \tag{8}$$

where am is the Jacobi elliptic amplitude, k is the corresponding modulus (associated with the applied magnetic field): k determines the detailed shape of the current distribution within the junction. When $k\ll 1$, the Josephson vortices form a densely packed array; the current distribution has the familiar sinusoidal shape with a wavelength $\Lambda=\pi k\overline{\lambda}_J$. As k increases, the spatial period of the lattice is given by $\Lambda=2k\overline{\lambda}_J K(k)$, where $K(k)$ is the complete elliptic integral of the first kind. The magnetic interjunction coupling is described by the interaction Hamiltonian, $H_{\rm in}$. Since the coupling constant η is negative, the interaction between fluxons in different barriers is repulsive. By minimizing the total energy, the relative spatial displacement of the fluxon positions in the two barriers is shown to be[12]

$$X_2^0-X_1^0=k\overline{\lambda}_J K(k). \tag{9}$$

As a result, if more than two fluxons are present, the fluxons in the two junctions will form a triangular lattice as schematically shown in the left inset in Fig. 1.

From the above analysis, the anomalous I_c vs H dependence shown in Figs. 1 and 2 can be understood qualitatively. If the barrier energies for both junctions in the stack are identical, the magnetic field distribution is symmetric with respect to the $Z=0$ plane (see the left inset in Fig. 1) when $\Phi<\Phi_0$; for this case, an in-phase ($\phi_1=\phi_2$) solution to Eqs. (2) is adequate. This symmetry breaks down when $\Phi>\Phi_0$.[13] Since the interaction between fluxons in the neighboring junctions is repulsive, if there are two Josephson vortices present, the total free energy will be minimized when the two vortices, one in each barrier, have a relative displacement in the x direction;[14] at high field it would be of order half the vortex spacing. The additional phase modulation in the z direction results in a more rapid field modulation in the x direction; the effective magnetic length $d_{\rm eff}$ becomes larger than d_+ given by Eq. (5a), resulting in a smaller oscillation period.

On the other hand, if the maximum Josephson supercurrents for the two junctions in the stack are not equal, due to the difference between the two barrier free energies, the in-phase solution is absent when $\Phi<\Phi_0$; when $\Phi>\Phi_0$, the fluxons can reside in the junction having the smaller barrier energy. As a result, the I_c vs H characteristic exhibits no transition in the low-field region; i.e., the behavior resembles that of a single junction. This is the case observed in sample C (see Fig. 3).

In the spirit of the above analysis, we can semiquantitatively discuss the I_c vs H data for sample A which is in the small junction limit. In this limit, $k\to 0$, $K(k)\to\pi/2$, and $k\overline{\lambda}_J=\Phi_0/\pi d_{\rm eff}H$;[1] from Eq. (7) we have

$$d_{\rm eff}=d_+d_-/d. \tag{10}$$

We may then use a function form similar to Eq. (1) to deduce the effective magnetic length. We note that when $\Phi<\Phi_0$, I_c should depend on H according to Eq. (1) with $y=\pi H/H_0$. The corresponding fit yields the characteristic field H_0. To fit the data for $\Phi>\Phi_0$, we introduce a fitting

parameter ν to account for the change in the effective magnetic length $d_{\rm eff}$, i.e., in Eq. (1) we use

$$y=\pi[\nu H/H_0-(\nu-1)]. \tag{11}$$

A phase amounting to $\pi(\nu-1)$ is introduced in expression (11) to model the phase shift associated with the addition of the extra fluxon.[15] Obviously, when $H=H_0$, the first current minima are recovered. By means of a least squares optimization procedure the fitting yields $\nu=d_{\rm eff}/d_+=1.51$. The I_c vs H curve calculated from Eqs. (1) and (11) using $\nu=1$ for $H<H_0$ and $\nu=1.51$ for $H>H_0$ is shown in Fig. 1 as the solid line. The agreement between the theoretical and experimental results is satisfactory.

The above argument is further supported by comparing the measured characteristic field H_0(B) (for sample B) and H_0(D) (for sample D). Experimentally, we find $H_0(\mathrm{B})/H_0(\mathrm{D})\approx 1.4$. In the small junction limit, using a $\sim$15 Å, $\lambda_L\sim$800 Å, the theoretical ratio $H_0(\mathrm{B})/H_0(\mathrm{D})=d_0/d_+=(a+2\lambda_L)/d_+\approx 1.6$. Therefore, $\phi_1\approx\phi_2$ is a good approximation when $\Phi<\Phi_0$. When $\Phi>\Phi_0$, the effective magnetic length is given by Eq. (10); hence $d_{\rm eff}/d_+=d_-/d\approx 1.68$, which is close to the observed ratio $\nu=d_{\rm eff}/d_+=1.51$. Using d_+ given by Eq. (5a), it can be shown that the lower critical field H_{c1} of a two-junction stack is[1]

$$H_{c1}=(2/\pi)(2\Phi_0 J_c/\pi\mu_0 d_+)^{1/2}=(2/\pi)(2LH_0J_c/\pi)^{1/2}. \tag{12}$$

Clearly, the H_{c1} of a two-junction stack is larger than that of a comparable single junction. We also note that H_0 decreases with T (see Fig. 5). However, the fitting parameter ν depends on T only weakly.

In summary, we have observed an anomalous I_c vs H dependence in Josephson junction stacks consisting of two junctions having identical Josephson supercurrents. The observations are consistent with a structural phase transformation involving a relative displacement of the fluxon positions in the two junctions which occurs with increasing H.

We are grateful to A. Patashinski for valuable discussions and E. D. Rippert, C. Thomas, and S. Maglic for assistance. This work was supported by NASA Innovative Research Project Program under Contract No. NAGW-2859, and the Northwestern Materials Research Center under NSF Grant DMR91-20501.

[1] A. Barone and G. Paterno, *Physics and Applications of the Josephson Effect* (Wiley, New York, 1982).
[2] C. S. Owen and D. J. Scalapino, Phys. Rev. **164**, 538 (1967).
[3] S. Sakai, P. Bodin, and N. F. Pedersen, J. Appl. Phys. **73**, 2411 (1993).
[4] S. Sakai, A. V. Ustinov, H. Kohlstedt, A. Petoaglia, and N. F. Pedersen, Phys. Rev. B **50**, 12 905 (1994).
[5] P. R. Auvil and J. B. Ketterson, J. Appl. Phys. **61**, 1957 (1987).
[6] S. N. Song, P. R. Auvil, and J. B. Ketterson, IEEE Trans. Magn. **MAG-23**, 1154 (1987).
[7] A. V. Ustinov, H. Kohlstedt, and C. Heiden, Appl. Phys. Lett. **65**, 1457 (1994).
[8] H. Kroger, L. N. Smith, and D. W. Jillier, Appl. Phys. Lett. **39**, 280 (1981).
[9] S. N. Song and J. B. Ketterson, Phys. Lett. A **208**, 150 (1995).
[10] M. B. Mineev, G. S. Mkrtchyan, and V. V. Schimdt, J. Low Temp. Phys. **45**, 497 (1981).
[11] N. Grønbech-Jensen, M. R. Samuelsen, P. S. Lomdahl, and J. A. Blackburn, Phys. Rev. B **42**, 3976 (1990).
[12] Y. S. Kivshar and T. K. Soboleva, Phys. Rev. B **42**, 2655 (1990).
[13] This is demonstrated by the observed behavior of I_{c1} vs H which differs from I_c vs H. For reference, see also H. Amin, M. G. Blamire, and J. E. Evetts, IEEE Trans. Appl. Supercond. **3**, 2204 (1993).
[14] Expanding Eq. (8) in power series and assuming the relative displacement of the two fluxons in the two barriers is x_0, the total energy E, calculated from Eq. (6), has a Ginzburg-Landau form: $E=E_0+\alpha x_0^2+(\beta/2)x_0^4$, where E_0 is a constant, the parameter α (depending on L, η, and H) can be negative, and β is always positive.
[15] Equation (11) may be justified by expanding Eq. (8) to the cubic term in x and calculating the resulting I_c.